

SCD1 deficiency protects mice against ethanol-induced liver injury

Mohamed A. Lounis¹, Quentin Escoula¹, Cathy Veillette¹, Karl-F. Bergeron¹, James M. Ntambi² and Catherine Mounier^{1*}

¹BioMed Research Center, Biological Sciences Department, University of Quebec in Montreal, Montreal, PQ, Canada H2X 1Y4

²Nutritional Sciences Department and Biochemistry Department, University of Wisconsin-Madison, Madison, WI, USA 53706

* corresponding author

Contact information:

Catherine Mounier, Biological Sciences Department, University of Quebec in Montreal, Montreal, PQ, Canada H2X 1Y4, 1-514-897-3000 extension 8912, mounier.catherine@uqam.ca

Abstract

Stearoyl-CoA desaturase 1 (SCD1) is a delta-9 fatty acid desaturase that catalyzes the synthesis of mono-unsaturated fatty acids (MUFA). SCD1 is a critical control point regulating hepatic lipid synthesis and β -oxidation. *Scd1* KO mice are resistant to the development of diet-induced non-alcoholic fatty liver disease (NAFLD). Using a chronic-binge protocol of ethanol-mediated liver injury, we aimed to determine if these KO mice are also resistant to the development of alcoholic fatty liver disease (AFLD).

Mice fed a low-fat diet (especially low in MUFA) containing 5% ethanol for 10 days, followed by a single ethanol (5g/kg) gavage, developed severe liver injury manifesting as hepatic steatosis. This was associated with an increase in *de novo* lipogenesis and inflammation. Using this model, we show that *Scd1* KO mice are resistant to the development of AFLD. *Scd1* KO mice do not show accumulation of hepatic triglycerides, activation of *de novo* lipogenesis nor elevation of cytokines or other pro-inflammatory markers. Incubating HepG2 cells with a SCD1 inhibitor induced a similar resistance to the effect of ethanol, confirming a role for SCD1 activity in mediating ethanol-induced hepatic injury.

Taken together, our study shows that SCD1 is a key player in the development of AFLD and associated deleterious effects, and suggests SCD1 inhibition as a therapeutic option for the treatment of this hepatic disease.

Keywords: alcoholic fatty liver disease, SCD1, *de novo* lipogenesis, inflammation

1. Introduction

Alcohol consumption and abuse is a risk factor of chronic disease worldwide and has long been identified as a major risk factor for all liver diseases (1). Liver diseases induced by ethanol abuse ranges from simple fatty liver to more severe forms of liver injury such as alcoholic hepatitis, cirrhosis and hepatocellular carcinoma (2, 3). A fatty liver, also known as alcoholic fatty liver disease (AFLD), is the earliest sign of ethanol-induced liver injury. This fat accumulation (i.e., steatosis) is usually accompanied by inflammation (4). AFLD occurs in 80% of heavy drinkers who consume an excess of 80g ethanol per day (5). This state is usually asymptomatic and can be reversed after 4 to 6 weeks of abstinence (6). However, continued heavy ethanol consumption increases by 30% the risk of progression to cirrhosis (7). Unfortunately, 5-15% of patients with AFLD develop fibrosis and cirrhosis despite abstinence (8).

Approximately 90% of ingested ethanol is metabolized in the liver (4). Ethanol is first oxidized to acetaldehyde by alcohol dehydrogenase and partly metabolized by cytochrome P-450 and catalase in hepatocyte microsomes and peroxisomes, respectively (4). Acetaldehyde is the major toxin in ethanol-induced liver injury, causing cellular damage, inflammation and fibrosis (9). Acetaldehyde also increases the redox ratio of nicotinamide adenine dinucleotide (NADH/NAD⁺) leading to a reduction of fatty acid β -oxidation through a reduction of PPAR α activity (4, 10). Activation of hepatic lipogenesis is another important biochemical characteristic of hepatic steatosis in AFLD development (11). *You* and collaborators have shown that ethanol induces fatty acid synthesis by acetaldehyde-mediated activation of the sterol regulatory element-binding protein (SREBP)-1 (12). Notably, SREBP-1 plays a central role in lipid metabolism by regulating the transcription of genes involved in hepatic lipid synthesis such as SREBP itself, ACC, FAS, and SCD1 (13). Acetaldehyde is then converted to acetate by acetaldehyde dehydrogenase (ALDH) in mitochondria of hepatocytes (9). High hepatic levels of acetate, the main substrate of ACC, can lead to the formation of acetyl-CoA in hepatocytes (14). In addition to lipid accumulation, the production of TNF- α is one of the earliest responses to ethanol-induced liver injury (15). TNF- α , a mediator of the mammalian inflammatory response, up-regulates hepatic SREBP mRNA expression,

activates its maturation and reduces PPAR α expression (4). Taken together, all these modifications lead to the aggravation of liver injury (4).

SCD1 is a delta-9 fatty acid desaturase that catalyzes the synthesis of 16:1(n-7) and 18:1(n-9) mono-unsaturated fatty acids (MUFA). SCD1 is a key enzyme in the regulation of hepatic lipogenesis and β -oxidation of lipids (16). Increases in the hepatic desaturation index resulting from elevated SCD1 expression and activity have been associated with non-alcoholic fatty liver (NAFLD) and metabolic syndrome (17). Several studies have shown that *Scd1*-deficient mice are protected against obesity and NAFLD (18, 19). *Scd1* KO mice have reduced lipid synthesis and enhanced β -oxidation of lipids, as well as increased thermogenesis and insulin sensitivity in various tissues, including the liver. These metabolic changes protect *Scd1* KO mice from a variety of dietary, pharmacological, and genetic conditions that promote hepatic steatosis.

Ethanol induces an increase in *de novo* lipogenesis via increased expression of key genes implicated in lipid metabolism (12). Due to its central role in hepatic lipid metabolism and its implication in the development of NAFLD (4), we evaluated the role of *Scd1* in the development of AFLD. We show that *Scd1* KO mice are completely protected against AFLD, suggesting that decreasing SCD1 activity can offer a new therapeutic strategy for the treatment of this disease.

2. Materials and Methods

2.1 Mice

Wild-type (WT) C57BL/6N mice were purchased from Charles River laboratories (Senneville, Canada). *Scd1* knockout (*Scd1* KO) mice in the C57BL/6N background originated from the Ntambi laboratory (University of Wisconsin-Madison, Madison, USA) and were generated in the University of Quebec in Montreal (UQAM) animal facilities. Only male mice were used in the study. The UQAM Animal Care and Use Committee approved all animal experimental protocols.

2.2 Chronic + binge protocol of alcoholic fatty liver disease induction

Twelve week-old male WT and *Scd1* KO mice were acclimated to a low-fat liquid control diet (AIN-76 (F1268); Bio-Serv, Frenchtown, USA) for 5 days. Thereafter, the animals were divided in four groups and divided into 2 or 3 mice per cage: WT with control diet (CTRL) (n=8), *Scd1* KO with control diet (*Scd1* KO) (n=5), WT with ethanol diet (EtOH) (n=8) and *Scd1* KO with ethanol diet (*Scd1* KO EtOH) (n=8). The ethanol groups (EtOH and *Scd1* KO EtOH) were fed a liquid diet (AIN-76 (F1436); Bio-Serv, Frenchtown, USA) containing 5% ethanol for 10 days while the CTRL group was maintained on the control diet. The caloric breakdown and fatty acid composition of these diets is described in **Table 1**. At day 11, mice in EtOH groups were gavaged a single dose of EtOH (5g/kg body weight, 31.5% solution), whereas mice in the control group were gavaged an isocaloric dose of dextrin maltose (45% solution). The gavage was always performed in the early morning. After gavage, mice were kept on control or EtOH diet for an additional 9h. During this time, the animals were kept on a warm electric blanket. After gavage, mice were slow moving, but conscious and regained normal behavior within 4-6h. The mice were euthanized 9h after gavage, when ALT and AST serum levels reach their peak (20).

2.3 Plasma transaminase assays

Blood was collected from mice by cardiac exsanguination in collection tubes containing 10 IU/ml Heparin. The blood was then centrifuged for 10min at 200g and the plasma was

collected for subsequent analysis. Aspartate transaminase (AST) and alanine transaminase (ALT) activities were measured using a Beckman DxC automated Monarch device (Biochemical laboratory, Notre-Dame Hospital, Montréal, Canada).

2.4 Liver histology

To detect fat deposition in the liver, frozen samples of livers were embedded in Optimal Cutting Temperature compound (OCT) (Fisher Scientific, Hampton, USA), sectioned (4-8 μ m) using a cryostat (Leica Biosystems, Wetzlar, Germany) and fixed for 10min in 4% paraformaldehyde. Then sections were stained with Oil Red-O (Sigma-Aldrich, Saint Louis, USA) for lipid accumulation and nuclei were lightly stained with Hematoxylin. Hematoxylin and Eosin (H&E) staining was used to evaluate neutrophil infiltration (21). Images were acquired with an A1 Nikon microscope using a 20X objective lens and a color camera.

2.5 Immunofluorescence

Immunofluorescence was used to evaluate the expression of F4/80, a macrophage marker. We used 8 μ m sections of livers from different groups as described above. Sections were then permeabilized for 10min using PBS 1X containing 0.25% Triton-X100 (PBST), blocked for 30min in 1% Bovine serum albumin (BSA) in PBST and finally incubated with Alexa Fluor 647 F4/80 antibody (1:250) (BioLegend, London, UK). Nuclei were then stained with DAPI and images were acquired with an A1 Nikon confocal microscope using a 20X objective lens.

2.6 Triglyceride assay

Concentration of liver triglycerides was determined using a colorimetric assay kit from Cayman Chemical (Ann Arbor, USA). Briefly, 200mg of liver tissue was homogenized in 1ml of Standard Diluent containing cOMplete protease inhibitor cocktail (Sigma-Aldrich, Saint Louis, USA). The homogenate was then centrifuged at 4°C for 10min at 10,000g. The supernatant was collected and hepatic triglycerides were measured by enzymatic hydrolysis of triglycerides to glycerol and free fatty acids, followed by colorimetric measurement (at 540nm wavelength) of glycerol. Values for hepatic triglycerides were

expressed as mg of triglyceride per g of liver tissue.

2.7 HepG2 cell culture

HepG2, a human hepatoma cell line, was obtained from ATCC (Manassas, USA) and maintained in Eagles minimum essential medium (EMEM; Wisent, St-Jean-Baptiste, Canada) supplemented with 10% fetal bovine serum (Life Technologies, Grand Island, USA). Twenty-four hours before treatments, cells were starved in serum free medium. Ethanol-induced injury was achieved by exposing cells to EtOH (50mM) in serum free medium for a total of 48h, the last 24h of which were spent in the presence of 1 μ M SCD1 inhibitor A939572 (Biofine, Vancouver, Canada) where appropriate.

2.8 Lipid droplet imaging

Control and ethanol-treated HepG2 cells were washed three times with ice-cold 1X PBS and fixed in 4% paraformaldehyde for 30min. Lipid droplets (LDs) were stained for 10min with 1 μ g/ml Bodipy 493/503 (Life Technologies, Grand Island, USA). Fluorescence was visualized using a Nikon A1 confocal microscope using a 40X objective lens.

2.9 Real-time PCR analysis

Total RNA was isolated from mice liver and HepG2 cells using the Trizol reagent (Fisher Scientific, Hampton, USA) and according to the manufacturer's protocol. One μ g of total RNA was reverse transcribed into complementary DNA (cDNA) at 42°C for 1h using dT₁₈ oligonucleotide and SuperScript II reverse transcriptase according to the manufacturer's protocol (Life Technologies, Grand Island, USA). Quantitative real-time PCR (qPCR) was performed using a PowerUp™ SYBR™ Green Master Mix (Life Technologies, Grand Island, USA) to quantify the mRNA levels of genes implicated in *de novo* lipogenesis and inflammation. Sequences of the primers used are listed in **Table 2**. The PCR amplification reactions were performed in a Roche LightCycler 480 Instrument (Penzberg, Germany). Data were normalized using the housekeeping gene HPRT1 and expressed as fold changes relative to control samples using the comparative delta-Ct ($\Delta\Delta$ Ct) method.

2.10 Western blot analysis

Cold PBS-washed liver tissues and HepG2 cells were homogenized in RIPA buffer containing 0.1mM PMSF and 1% of cOmplete protease inhibitor (Sigma-Aldrich, Saint Louis, USA). The homogenates were then centrifuged at 15 000g 15min at 4 °C, and the supernatant collected. The protein concentrations were determined using a protein assay reagent (Bio-Rad Laboratories, Hercules, USA). Proteins were separated by 10% sodium dodecyl sulfate-polyacrylamide gel electrophoresis and transferred to PVDF membranes (Bio-Rad Laboratories, Hercules, USA). The membranes were blocked with 5% non-fat skim milk and incubated with either an anti-NF- κ B (1:500; Santa Cruz Biotechnology, Dallas, USA), an anti-SREBP-1 (1:500; Santa Cruz Biotechnology, Dallas, USA), an anti-CPT1 (1:1000; Abcam, Cambridge, USA) or an anti-PPAR α (1:1000; Cell Signaling, Danvers, USA) antibody. After incubation, the membranes were washed in 1X PBS + 0.1% Tween and incubated with anti-mouse or anti-rabbit horseradish peroxidase-conjugated secondary antibodies (1:5000; Cell Signaling Technology, Danvers, USA). The immunoreactive bands were revealed by chemiluminescence (Millipore, Billerica, USA) and using a chemi-luminometer (FusionFX, Collegien, France).

2.11 Statistical Analysis

Data are expressed as mean \pm SD. To compare values between three or more groups, a one-way ANOVA was performed and followed by a Tukey's post hoc test. Comparison tests with p -values < 0.05 were considered significantly different.

3. Results

3.1 Chronic + binge ethanol feeding leads to AFLD in mice

A low-fat liquid diet was used to administer ethanol to mice. This diet (detailed in **Table 1**) contains a lower amount of MUFA (3.7g/L) compared to other commercially available liquid diets. Using this diet in a chronic + binge protocol of ethanol (EtOH) abuse, leads to mice with severe liver injury characterized by changes in consistency and color. The livers of the EtOH group appear pale, yellow and granular compared to controls (**Fig.1A**), and there is a significant increase in the gallbladder content of the EtOH group (*data not shown*). Interestingly, important fat accumulation (**Fig.1B**) and neutrophil infiltration (**Fig.1C**) are specifically observed in liver sections of the EtOH group. We also observed high AST (443 *versus* 97 IU/L for CTRL) (**Fig.2A**) and ALT (141 *versus* 31 IU/L for CTRL) (**Fig.2B**) plasmatic levels, as well as a 3.2-fold increase in hepatic triglycerides (TG) (**Fig.2C**) and 1.6-fold increase of the hepatic index (**Fig.2D**).

We observed a continuous decrease in body weight during EtOH consumption (**Fig.3A**). This was echoed by a smaller final body weight (**Fig.3B**) and is probably the result of a decrease in food intake in EtOH-fed mice (**Fig.3C**). Altogether, these features demonstrate the induction of AFLD by ethanol feeding.

3.2 *Scd1* deficiency protects mice against AFLD

To characterize the role of *Scd1* in the development of AFLD, we used the chronic + binge ethanol feeding protocol on *Scd1* KO mice. As for the EtOH group, the body weight of *Scd1* KO EtOH-fed mice steadily decreases on the EtOH diet (**Fig.3**). As previously mentioned, livers of the EtOH group (WT mice) show significant changes in colour and aspect (**Fig.1A**). Interestingly, livers of the *Scd1* KO mice fed with EtOH appear normal and very similar to the livers of the control groups (CTRL and *Scd1* KO) (**Fig.1A**). As expected, a large number of Red O-stained lipid droplets are seen in the livers of WT mice fed with EtOH while little staining is visible in the livers of *Scd1* KO EtOH mice (**Fig.1B**). Hematoxylin and Eosin staining reveals neutrophil infiltrations in the liver of WT mice fed with EtOH while no significant neutrophil infiltration can be detected in the *Scd1* KO EtOH mice nor in the control groups (**Fig.1C**). Neutrophil

infiltrations in EtOH-injured WT livers are associated with an increased number of F4/80⁺ macrophages (**Fig.1D**).

AST and ALT serum levels (**Fig.2A,B**) are very low in *Scd1* KO mice compared to WT mice fed with EtOH (160 and 65 IU/L *versus* 443 and 141 IU/L for AST and ALT, respectively). Hepatic triglyceride (**Fig.2C**) and hepatic index (HI) (**Fig.2D**) values are also very low in the *Scd1* KO EtOH group compared to EtOH only (32mg/g and 2.55% *versus* 136mg/g and 3.90%), and are actually similar to levels in both CTRL and *Scd1* KO control groups.

3.3 Effect of ethanol feeding on hepatic lipogenesis and β -oxidation

As lipid parameters are dramatically increased in the livers of EtOH-fed WT mice (**Figs.1B & 2C,D**), we measured the relative mRNA expression of key genes involved in *de novo* lipogenesis (DNL) such as *Srebp-1*, *Acc*, *Fas*, *Lxr α* and *Scd1* (22). As an increase in TG content may also results from a decrease in β -oxidation, the level of expression of key genes involved in this process were also examined (*Ppara α* and *Cpt1*) (22). We observed an increase in the expression of *Ppara α* and *Cpt1* in *Scd1* KO mice, as expected (18). Our results show that compared to control, EtOH feeding of WT mice leads to a significant increase in the expression of genes implicated in DNL (**Fig.4A**), while genes implicated in β -oxidation are decreased (**Fig.4B**). Remarkably, in EtOH-fed *Scd1* KO mouse livers, an increase in lipogenic gene expression is observed only for *Acc*, and it is less pronounced than in the EtOH group (**Fig.4A**). Moreover, the decrease in β -oxidation gene expression following EtOH-feeding is not seen in *Scd1* KO mice (**Fig.4B**).

3.4 *Scd1* deficiency protects mice against ethanol-induced inflammation

As the livers of EtOH-fed WT mice show several indications of inflammation (**Fig.1C,D**), we measured the relative mRNA expression of key genes involved in this process. An elevation of gene expression is seen for a number of pro-inflammatory cytokines (*Tnf- α* , *Il-6* and *Inf γ*) (**Fig.5A**), as well as for monocyte (*Mcp* and *Ccr2*; **Fig.5B**) and macrophage (F4/80; **Fig.5C**) markers, in the livers of EtOH-fed WT mice

compared to CTRL and *Scd1* KO control groups. Remarkably, *Scd1* KO mice fed with EtOH show a much less severe upregulation of these inflammatory markers, notably in markers of monocyte/macrophage infiltration (**Fig.5**).

3.5 SCD1 inhibition protects HepG2 cells against ethanol-induced injury

In order to confirm that our observations in *Scd1* KO mouse livers are associated with a decrease in SCD1 activity, and to explore the therapeutic potential of SCD1 inhibition, we treated HepG2 cells exposed to EtOH with an inhibitor of SCD1 activity. We show that a SCD1 inhibitor (1 μ M A939572) considerably reduces EtOH-mediated lipid droplet accumulation in HepG2 cells (**Fig.6A**). SREBP-1 mRNA and protein expression are elevated in EtOH-treated HepG2 cells. In the presence of a SCD1 inhibitor, SREBP-1 expression is lower than the one observed in EtOH-treated cells (**Fig.6B**), suggesting a prevention of DNL activation. PPAR α and CPT1 protein levels in HepG2 cells are diminished by EtOH-treatment. In presence of the SCD1 inhibitor, the expression of PPAR α and CPT1 remains elevated, suggesting high fatty acid oxidation (**Fig.6B**). Finally, the expression of inflammation markers TNF- α and NF- κ B in HepG2 is increased following EtOH treatment yet remains similar to control levels when SCD1 activity is inhibited (**Fig.6C**).

4. Discussion

In this study, we show that a murine liver injury characterized by significant steatosis and inflammation can be induced by an ethanol feeding protocol on a low-fat diet with very low MUFA content. Using this protocol, we demonstrate that *Scd1* KO mice are resistant to the development of ethanol-induced liver steatosis and inflammation. We also show that treatment with a SCD1 activity inhibitor can considerably reduce ethanol-induced damages in HepG2 cell cultures. These findings clearly demonstrate a central role for SCD1 in the development of AFLD and identify SCD1 as a potential therapeutic target for treatment of this disease.

Recently, Gao and collaborators developed a new chronic + binge ethanol feeding protocol for mice (20) that is highly relevant to AFLD as it mimics chronic human alcohol consumption combined with occasional binge drinking. This protocol generates a more severe liver injury, with increased lipid accumulation and inflammation as well as higher AST and ALT plasmatic levels, than other frequently used protocols. We used the same chronic + binge approach combined with a low-fat diet to induce liver injury in C57BL/6N mice (**Fig.1**). This low-fat AIN-76 diet contains very little MUFA (3.4g/L) (**Table 1**). Many studies, including those of Gao *et al.*, use the Lieber-De Carli 82 diet which contains 18% fat and 23.5g/L MUFA. As C16:1(n-7) and C18:1(n-9) (20, 23). MUFA are products of SCD1-mediated desaturation, it was important to limit the exogenous dietary contribution of these fatty acids in order to prevent compensation for the loss of SCD1 activity in KO mice.

Scd1 KO mice are protected against ethanol-induced fatty liver injury (**Figs.1-5**). Livers of *Scd1* KO ethanol-fed mice show a normal appearance (**Fig.1A**), very low lipid accumulation (**Figs.1B & 2C**) and no significant neutrophil or monocyte/macrophage infiltration (**Fig.1C,D**). However, we detect some hepatic injury via blood markers (AST and ALT; **Fig.2A,B**). The levels of hepatic fat accumulation in ethanol-fed *Scd1* KO mice are similar to non-alcohol and *Scd1* KO control groups, and are probably the result of the relatively small modulation in the expression of lipogenesis genes (*Srebp-1*, *Acc*, *Fas*,

Lxra and *Scd1*; **Fig.4A**) compared to the EtOH group. Ethanol treatment inhibits AMPK activity and lowers phosphorylation of ACC. Since these phosphorylation events are inhibiting, ACC activity is increased and DNL is induced in the presence of ethanol (24). However, when SCD1 is inhibited, AMPK activity is increased, resulting in inhibition of ACC activity and DNL (25). SCD1 deficiency also inhibits SREBP-1 expression and maturation, leading to a further decrease in DNL (26). The importance of SCD1 activity in DNL regulation may therefore explain the absence of hepatic steatosis observed in the ethanol-fed *Scd1* KO mice. These KO mice also show a significant increase in β -oxidation gene expression (*Ppara* and *Cpt1*), independently of ethanol feeding (**Fig.4B**). This is a typical trait of the *Scd1* KO model as this pattern has also been observed on other diets (18). This increase in hepatic lipid catabolism following SCD1 deficiency (25, 27) could also explain the absence of steatosis in ethanol-fed *Scd1* KO mice. In fact, an increase in β -oxidation can be sufficient to prevent fat deposition in the liver (26). Previous studies have yielded contradictory results concerning the effect of ethanol on SCD1 activity. In fact, Rao *et al.* showed a decrease in SCD1 activity in livers of ethanol-fed rats (28). At the opposite and in agreement with our observations, another study showed a Δ -9 activity increase in ethanol-fed micropigs (29). Similarly, more recent studies have shown that ethanol consumption increase MUFA and decrease SFA contents in human livers and in rat hepatocytes (30, 31).

Scd1 KO mice display a lower inflammation state than WT controls, as measured by hepatocyte production of pro-inflammatory cytokines TNF- α and IL-6 (**Fig.5A**). Moreover, monocyte/ macrophage infiltration markers are also lowered in *Scd1* KO mice livers (**Fig.5B,C**). This result is consistent with previous work showing a decrease in the expression of inflammation markers in white adipose tissue and macrophages of *Scd1* KO mice (32). Interestingly, the same study showed that treatment of macrophages from *Scd1* KO mice with C18:1(n-9) induces an increase in TNF- α and promotes inflammation (32). However, the molecular mechanism by which SCD1 regulates inflammation remains to be elucidated. Ethanol feeding of WT mice strongly induces the hepatic expression of cytokines (*Tnf- α* , *Il-6* and *Inf γ*) (**Fig.5A**). In EtOH-fed *Scd1* KO mice, the levels of these inflammation markers as well as macrophage/ monocyte infiltration markers (**Fig.5B,C**)

tend to rise compared to the *Scd1* KO group to reach levels similar to the ones measured in the CTRL group, with the exception of *Infy* that rises higher still (**Fig.5A**). The relatively low expression of inflammation and infiltration markers in EtOH-fed *Scd1* KO mice is echoed by an absence of neutrophil/ macrophage infiltration. This lack of neutrophil/ macrophage infiltration (**Fig.1C,D**) and of monocyte/ macrophage marker induction (**Fig.5B,C**) suggests an absence of hepatic inflammation in ethanol-fed *Scd1* KO mice. This absence of inflammation could contribute to the effect of *Scd1* deficiency on DNL and/or β -oxidation as TNF- α can induce SREBP-1 maturation and inhibit PPAR α expression, leading to an upregulation of DNL and a decrease in β -oxidation (4, 33).

To confirm that the ethanol-induced liver injury protection observed in *Scd1* KO mice is a consequence of a deficiency in SCD1 activity, we exposed ethanol-treated HepG2 cells to a SCD1 inhibitor. In adipocytes, this SCD1 inhibitor decreases DNL and inflammation, and increases fatty acid oxidation (34), features we observe in livers of *Scd1* KO mice. Interestingly, inhibition of SCD1 activity diminishes ethanol-induced lipid droplet accumulation (**Fig.6A**), DNL (SREPB-1; **Fig.6B**) and inflammation marker levels (**Fig.6C**), and rescues ethanol-induced fatty acid β -oxidation (CPT1 and PPAR α ; **Fig.6B**). It appears that all the major aspects of ethanol injury we quantified in mice (hepatic steatosis, lipid anabolism/catabolism, inflammation) are repeated in this *in vitro* model and are normalized by an inhibition of SCD1 activity.

Ethanol consumption induces an increase in the concentration of acetyl-CoA in hepatic cells (4), leading to increased DNL and decreased fatty acid β -oxidation. This is also associated with increased inflammation, manifesting as elevated cytokine levels and neutrophil/ macrophage infiltrations (**Fig.7A**). In contrast, in the absence of SCD1 expression or activity, these phenomena are almost absent (**Fig.7B**). As SCD1 desaturates SFA to form MUFA, This might be the result of a higher SFA content, and increased SFA/MUFA ratio. Diets enriched in SFA are protective against ethanol-induced liver injuries compared to diet enriched in unsaturated fatty acids (USF). Mice on a diet supplemented with saturated long chain fatty acids (palmitic acid (C16:0, 25%) and

stearic acid (C18:0, 85%)) develop a less severe ethanol-associated liver disease (35-37). These mice have reduced levels of hepatic injury, steatosis, and oxidative stress compared to ethanol-fed mice on a diet enriched in USF oleic acid (C18:1, 27%) and linoleic acid (C18:2, 60%) (38). The beneficial effect of a SFA-rich diet compared to an USF-rich diet, is attributed to the modulation of the hepatic Sirtuin- SREBP-1- histone H3 axis, resulting in the suppression of lipogenic genes via a reduction of SREBP maturation (39). However, the protective potential of saturated fatty acids in humans is less convincing. Recent studies have shown that a SFA-rich diet induces NAFLD in humans and could not be used as a therapy for treating fatty liver disease (32, 40). For this reason it would be best to find a molecular target to treat all forms of fatty liver disease (NAFLD and AFLD). There are similarities between AFLD and NAFLD. AFLD is caused by the formation and storage of TG in hepatocytes (41). Chronic alcohol consumption promotes steatosis by disrupting hepatic lipid metabolism via increased DNL and decreased β -oxidation (11). On the other hand, NAFLD is caused by an over-consumption of a high fat, high sugar diet saturating the adipose tissue. The excess fat is then stored in the liver (42). Intracellular lipid accumulation in NAFLD results from an imbalance between hepatic fatty acid uptake, lipid synthesis, lipid oxidation, and export through VLDL particles (43). *Scd1* deficiency in mice induces resistance to NAFLD (18) and AFLD development (this study), probably by increasing β -oxidation and decreasing DNL. This commonality implies that liver-targeted inhibition of SCD1 could be used to treat both NAFLD and AFLD.

In conclusion, mice submitted to a chronic + binge ethanol feeding protocol on a low MUFA diet display liver injury and inflammation. Importantly, SCD1 deficiency almost completely prevents the deleterious effect of ethanol consumption in mice, highlighting the central role of SCD1 in AFLD. Future studies are needed to determine if a direct inhibition of SCD1 activity can help treat this disease.

Acknowledgments

We wish to thank Dr. Pierre Olivier Héту (Notre, Dame Hospital, Université du Québec à Montréal, Canada) for the measurement of AST and AST serum levels. We also thank the employees of our animal facility for their help (Université du Québec à Montréal, Canada). The Discovery Grants Program of the National Science and Engineering Research Council of Canada (NSERC) funded this research. MAL is supported by a Fond de Recherche du Québec-Nature et Technologie (FRQNT) fellowship.

Conflict of interest

The authors declare that they have no conflicts of interest with the contents of this article.

Author contributions

MAL and CM designed the study. MAL performed most experiments. MAL and EQ performed the experiments shown in Figures 1 and 3. MAL and CV performed the experiments shown in Figure 6. MAL, KFB, JMN and CM analyzed the experiments and wrote the paper. All authors reviewed the results and approved the final version of the manuscript.

References

1. Williams JA, Manley S, Ding WX. New advances in molecular mechanisms and emerging therapeutic targets in alcoholic liver diseases. *World J Gastroenterol*. 2014;20(36):12908-33.
2. O'Shea RS, Dasarathy S, McCullough AJ, Practice Guideline Committee of the American Association for the Study of Liver D, Practice Parameters Committee of the American College of G. Alcoholic liver disease. *Hepatology*. 2010;51(1):307-28.
3. Lucey MR, Mathurin P, Morgan TR. Alcoholic hepatitis. *N Engl J Med*. 2009;360(26):2758-69.
4. Liu J. Ethanol and liver: recent insights into the mechanisms of ethanol-induced fatty liver. *World J Gastroenterol*. 2014;20(40):14672-85.
5. Levene AP, Goldin RD. The epidemiology, pathogenesis and histopathology of fatty liver disease. *Histopathology*. 2012;61(2):141-52.
6. Mendenhall CL. Anabolic steroid therapy as an adjunct to diet in alcoholic hepatic steatosis. *Am J Dig Dis*. 1968;13(9):783-91.
7. Teli MR, Day CP, Burt AD, Bennett MK, James OF. Determinants of progression to cirrhosis or fibrosis in pure alcoholic fatty liver. *Lancet*. 1995;346(8981):987-90.
8. Sorensen TI, Orholm M, Bentsen KD, Hoybye G, Eghoje K, Christoffersen P. Prospective evaluation of alcohol abuse and alcoholic liver injury in men as predictors of development of cirrhosis. *Lancet*. 1984;2(8397):241-4.
9. Mello T, Ceni E, Surrenti C, Galli A. Alcohol induced hepatic fibrosis: role of acetaldehyde. *Mol Aspects Med*. 2008;29(1-2):17-21.
10. Israel Y, Kalant H, Khanna JM, Orrego H, Phillips MJ, Stewart DJ. Ethanol metabolism, oxygen availability and alcohol induced liver damage. *Adv Exp Med Biol*. 1977;85A:343-58.
11. Louvet A, Mathurin P. Alcoholic liver disease: mechanisms of injury and targeted treatment. *Nat Rev Gastroenterol Hepatol*. 2015;12(4):231-42.
12. You M, Fischer M, Deeg MA, Crabb DW. Ethanol induces fatty acid synthesis pathways by activation of sterol regulatory element-binding protein (SREBP). *J Biol Chem*. 2002;277(32):29342-7.
13. Strable MS, Ntambi JM. Genetic control of de novo lipogenesis: role in diet-induced obesity. *Crit Rev Biochem Mol Biol*. 2010;45(3):199-214.
14. Yamashita H, Kaneyuki T, Tagawa K. Production of acetate in the liver and its utilization in peripheral tissues. *Biochim Biophys Acta*. 2001;1532(1-2):79-87.
15. Tilg H, Diehl AM. Cytokines in alcoholic and nonalcoholic steatohepatitis. *N Engl J Med*. 2000;343(20):1467-76.
16. Cohen P, Miyazaki M, Socci ND, Hagge-Greenberg A, Liedtke W, Soukas AA, et al. Role for stearoyl-CoA desaturase-1 in leptin-mediated weight loss. *Science*. 2002;297(5579):240-3.
17. Bjermo H, Riserus U. Role of hepatic desaturases in obesity-related metabolic disorders. *Curr Opin Clin Nutr Metab Care*. 2010;13(6):703-8.
18. Ntambi JM, Miyazaki M, Stoehr JP, Lan H, Kendziorski CM, Yandell BS, et al. Loss of stearoyl-CoA desaturase-1 function protects mice against adiposity. *Proc Natl Acad Sci U S A*. 2002;99(17):11482-6.

19. MacDonald ML, Singaraja RR, Bissada N, Ruddle P, Watts R, Karasinska JM, et al. Absence of stearoyl-CoA desaturase-1 ameliorates features of the metabolic syndrome in LDLR-deficient mice. *J Lipid Res.* 2008;49(1):217-29.
20. Bertola A, Mathews S, Ki SH, Wang H, Gao B. Mouse model of chronic and binge ethanol feeding (the NIAAA model). *Nat Protoc.* 2013;8(3):627-37.
21. Ki SH, Park O, Zheng M, Morales-Ibanez O, Kolls JK, Bataller R, et al. Interleukin-22 treatment ameliorates alcoholic liver injury in a murine model of chronic-binge ethanol feeding: role of signal transducer and activator of transcription 3. *Hepatology.* 2010;52(4):1291-300.
22. Berlanga A, Guiu-Jurado E, Porrás JA, Auguet T. Molecular pathways in non-alcoholic fatty liver disease. *Clin Exp Gastroenterol.* 2014;7:221-39.
23. Gao B, Bataller R. Alcoholic liver disease: pathogenesis and new therapeutic targets. *Gastroenterology.* 2011;141(5):1572-85.
24. You M, Matsumoto M, Pacold CM, Cho WK, Crabb DW. The role of AMP-activated protein kinase in the action of ethanol in the liver. *Gastroenterology.* 2004;127(6):1798-808.
25. Kim E, Lee JH, Ntambi JM, Hyun CK. Inhibition of stearoyl-CoA desaturase1 activates AMPK and exhibits beneficial lipid metabolic effects in vitro. *Eur J Pharmacol.* 2011;672(1-3):38-44.
26. Miyazaki M, Dobrzyn A, Man WC, Chu K, Sampath H, Kim HJ, et al. Stearoyl-CoA desaturase 1 gene expression is necessary for fructose-mediated induction of lipogenic gene expression by sterol regulatory element-binding protein-1c-dependent and -independent mechanisms. *J Biol Chem.* 2004;279(24):25164-71.
27. Miyazaki M, Flowers MT, Sampath H, Chu K, Otzelberger C, Liu X, et al. Hepatic stearoyl-CoA desaturase-1 deficiency protects mice from carbohydrate-induced adiposity and hepatic steatosis. *Cell Metab.* 2007;6(6):484-96.
28. Rao GA, Lew G, Larkin EC. Alcohol ingestion and levels of hepatic fatty acid synthetase and stearoyl-CoA desaturase activities in rats. *Lipids.* 1984;19(2):151-3.
29. Nakamura MT, Tang AB, Villanueva J, Halsted CH, Phinney SD. Selective reduction of delta 6 and delta 5 desaturase activities but not delta 9 desaturase in micropigs chronically fed ethanol. *J Clin Invest.* 1994;93(1):450-4.
30. Pawlosky RJ, Salem N, Jr. Perspectives on alcohol consumption: liver polyunsaturated fatty acids and essential fatty acid metabolism. *Alcohol.* 2004;34(1):27-33.
31. Retterstol K, Lund AM, Tverdal S, Cristophersen BO. Metabolism of some radiolabeled essential fatty acids in isolated rat hepatocytes is affected by dietary ethanol. *Alcohol.* 2000;21(1):19-26.
32. Petersson H, Arnlov J, Zethelius B, Riserus U. Serum fatty acid composition and insulin resistance are independently associated with liver fat markers in elderly men. *Diabetes Res Clin Pract.* 2010;87(3):379-84.
33. Tai ES, bin Ali A, Zhang Q, Loh LM, Tan CE, Retnam L, et al. Hepatic expression of PPARalpha, a molecular target of fibrates, is regulated during inflammation in a gender-specific manner. *FEBS Lett.* 2003;546(2-3):237-40.
34. Liu X, Strable MS, Ntambi JM. Stearoyl CoA desaturase 1: role in cellular inflammation and stress. *Adv Nutr.* 2011;2(1):15-22.

35. Kirpich IA, Miller ME, Cave MC, Joshi-Barve S, McClain CJ. Alcoholic Liver Disease: Update on the Role of Dietary Fat. *Biomolecules*. 2016;6(1).
36. Nanji AA. Role of different dietary fatty acids in the pathogenesis of experimental alcoholic liver disease. *Alcohol*. 2004;34(1):21-5.
37. Ronis MJ, Korourian S, Zipperman M, Hakkak R, Badger TM. Dietary saturated fat reduces alcoholic hepatotoxicity in rats by altering fatty acid metabolism and membrane composition. *J Nutr*. 2004;134(4):904-12.
38. Chen P, Torralba M, Tan J, Embree M, Zengler K, Starkel P, et al. Supplementation of saturated long-chain fatty acids maintains intestinal eubiosis and reduces ethanol-induced liver injury in mice. *Gastroenterology*. 2015;148(1):203-14 e16.
39. You M, Cao Q, Liang X, Ajmo JM, Ness GC. Mammalian sirtuin 1 is involved in the protective action of dietary saturated fat against alcoholic fatty liver in mice. *J Nutr*. 2008;138(3):497-501.
40. Rosqvist F, Iggman D, Kullberg J, Cedernaes J, Johansson HE, Larsson A, et al. Overfeeding polyunsaturated and saturated fat causes distinct effects on liver and visceral fat accumulation in humans. *Diabetes*. 2014;63(7):2356-68.
41. Lieber CS. Hepatic, metabolic and toxic effects of ethanol: 1991 update. *Alcohol Clin Exp Res*. 1991;15(4):573-92.
42. Musso G, Gambino R, Cassader M. Recent insights into hepatic lipid metabolism in non-alcoholic fatty liver disease (NAFLD). *Prog Lipid Res*. 2009;48(1):1-26.
43. Koo SH. Nonalcoholic fatty liver disease: molecular mechanisms for the hepatic steatosis. *Clin Mol Hepatol*. 2013;19(3):210-5.

Table 1. Caloric breakdown and fatty acid composition of liquid diets

	Control liquid diet		Ethanol liquid diet	
	AIN-76 (Bio-Serv #F1268)		AIN-76 (Bio-Serv #F1436)	
Caloric breakdown				
	kcal/L	% kcal	kcal/L	% kcal
protein	180	18.0	173	17.3
fat	125	12.5	124	12.4
<i>carbohydrate</i>	<i>695</i>	<i>69.5</i>	<i>348</i>	<i>34.8</i>
<i>ethanol</i>	-	-	355	35.5
total	1000	100	1000	100
Fatty acid composition				
	g/L	g/100g total fat	g/L	g/100g total fat
saturated	1.7	13.3	1.7	13.3
monounsaturated	3.7	28.9	3.7	28.9
polyunsaturated	7.4	57.8	7.4	57.8
total	12.8	100	12.8	100

Table 2. Primers sequences for mouse and human genes used in real-time PCR

Species	genes	Forward primer (5'...3')	Reverse primer (5'...3')
Mouse	SREBP-1	GAGGCCAAGCTTTGGACCTGG	CCTGCCTTCAGGCTTCTCAGG
	FAS	ATTGCATCAAGCAAGTGCAG	GAGCCGTCAAACAGGAAGAG
	ACC	TGAAGGGCTACCTCTAATG	TCACAACCCAAGAACCAC
	SCD-1	CTGCCTCTTCGGGATTTTCTACT	GCCCATTCGTACACGTGATTC
	LXR α	ATTAAGGAAGAGGGGCAGGA	GCTGAGCACGTTGTAGTGGA
	PPAR α	CTGCAGAGCAACCATCCAGAT	GCCGAAGGTCCACCATTTT
	CPT-1	TCCATGCATACCAAAGTGGA	TGGTAGGAGAGCAGCACCTT
	TNF- α	AAGCCTGTAGCCCACGTCGTA	AGGTACAACCCATCGGCTGG
	IFN- γ	TAGCCAAGACTGTGATTGCGG	AGACATCTCCTCCCATCAGCAG
	IL-6	TCCATCCAGTTGCCTTCTTG	TTCCACGATTTCCCAGAGAAC
	MCP-1	TCAGCCAGATGCAGTTAACGC	TCTGGACCCATTCTTCTTGG
	CCR2	ATGCAAGTTCAGCTGCCTGC	ATGCCGTGGATGAACTGAGG
	F4/80	GGAAAGCACCATGTTAGCTGC	CCTCTGGCTGCCAAGTTAATG
	HPRT	TCAGTCAACGGGGGACATAAA	GGGGCTGTACTGCTTAACCAG
Human	SREBP-1	ACAGTGACTTCCCTGGCCTAT	GCATGGACGGGTACATCTTCAA
	TNF- α	CCTCTCTCTAATCAGCCCTCTG	GAGGACCTGGGAGTAGATGAG
	HPRT1	CCTGGCGTCGTGATTAGTGAT	AGACG TTCAGT CCTGTCCATAA

Figure Legends

Figure 1. Genetic deletion of *Scd1* protects mice from ethanol feeding-induced liver injury

The chronic + binge protocol was used to induce AFLD and mouse livers were dissected for analysis. (A) Representative pictures of mouse livers in the abdominal cavity. (B) Oil Red-O staining of hepatic tissue sections showing fat accumulation. Hematoxylin was used as a nuclear counterstain. (C) Hematoxylin and Eosin (H&E) staining of liver sections; inset (2X zoom) shows neutrophil infiltration in the EtOH group. (D) Immunofluorescence staining of F4/80⁺ cells (red) in liver sections. Cell nuclei are shown in blue. Scale bars: 10µm. CTRL: control mice, *Scd1* KO: *Scd1* knockout mice, EtOH: ethanol-fed mice, *Scd1* KO EtOH: *Scd1* knockout mice fed with ethanol. Values represent mean ± SD (n= 5-8). A one-way ANOVA was used to compare groups, *** $p < 0.001$.

Figure 2. Effect of ethanol feeding on hepatic metabolic characteristics

The plasma and livers of mice on the chronic + binge protocol were used to measure several hepatic health parameters. (A,B) Concentrations of serum AST and ALT. (C) Hepatic triglyceride concentrations. (D) Hepatic index (%), calculated by dividing the liver weight by the body weight. CTRL: control, EtOH: ethanol-fed, *Scd1* KO: *Scd1* knockout. Values represent mean ± SD (n= 5-8). A one-way ANOVA was used to compare groups, ** $p < 0.01$; *** $p < 0.001$.

Figure 3. Effect of ethanol consumption on body weight and food intake

AFLD was induced by the chronic + binge protocol after a 5 day acclimation period on the liquid diet. (A) Daily body weight, normalized to the initial body weight of control animals. (B) Body weight on the last day of the protocol. (C) Average food intake (ml) per mouse per day. CTRL: control, EtOH: ethanol-fed, *Scd1* KO: *Scd1* knockout. Values represent mean ± SD (n= 5-8). A one-way ANOVA was used to compare groups, * $p < 0.05$; ** $p < 0.01$; *** $p < 0.001$.

Figure 4. Effect of ethanol feeding on hepatic lipogenic and β -oxydation gene expression

RNA from the livers of mice on the chronic + binge protocol was used to measure expression (by qPCR) of genes associated with lipogenesis (A) and β -oxidation (B). CTRL: control, EtOH: ethanol-fed, *Scd1* KO: *Scd1* knockout. Values represent mean \pm SD (n=5-8). A one-way ANOVA was used to compare groups, * $p < 0.05$; ** $p < 0.01$; *** $p < 0.001$.

Figure 5. Effect of ethanol feeding on expression of hepatic inflammation-related genes

RNA from the livers of mice on the chronic + binge protocol was used to measure expression (by qPCR) of genes associated with inflammation: (A) pro-inflammatory cytokines TNF- α , INF γ and IL-6, (B) monocyte markers CCR2 and MCP, and (C) macrophage marker F4/80. CTRL: control, EtOH: ethanol-fed, *Scd1* KO: *Scd1* knockout. Values represent mean \pm SD (n=5-8). A one-way ANOVA was used to compare groups, * $p < 0.05$; ** $p < 0.01$; *** $p < 0.001$.

Figure 6. Effect of SCD1 inhibition on ethanol-treated HepG2 cells

Serum-starved HepG2 cells were incubated or not with 50mM ethanol (EtOH) for 24h then a specific SCD1 inhibitor (A939572; 1 μ M) was added or not for 24h, for a total treatment time of 48h. (A) Treated cells were stained with Bodipy 493/503 to visualize lipid droplets. Scale bars: 20 μ m. Expression (measured by Western blot and qPCR) of key genes implicated in lipid metabolism (B) and inflammation (C). p: precursor, m: mature, CTRL: control, EtOH: ethanol-treated. Values represent mean \pm SD (n=5). A one-way ANOVA was used to compare groups, * $p < 0.05$; ** $p < 0.01$; *** $p < 0.001$.

Figure 7. Schematic representation of the role of SCD1 in the development of alcoholic hepatic steatosis

(A) In the normal liver, ethanol consumption induces an increase in acetyl-CoA, which triggers fatty acid synthesis through elevated expression of key *de novo* lipogenesis (DNL) genes (SREBP, ACC, SCD1, FAS...), and a decrease in β -oxidation of fatty

acids. Ethanol induces local inflammation by prompting the expression of pro-inflammatory genes (such as TNF- α) as well as the infiltration of neutrophils and monocytes/macrophages. **(B)** Scd1 deficient mice are protected against ethanol-induced liver injury. The liver of Scd1 deficient mice shows no increase in DNL while β -oxidation is increased. This is could be due to a higher SFA/MUFA ratio since the Scd1 desaturase is not producing MUFA. The expression of pro-inflammatory genes remains unchanged.

Figure 1

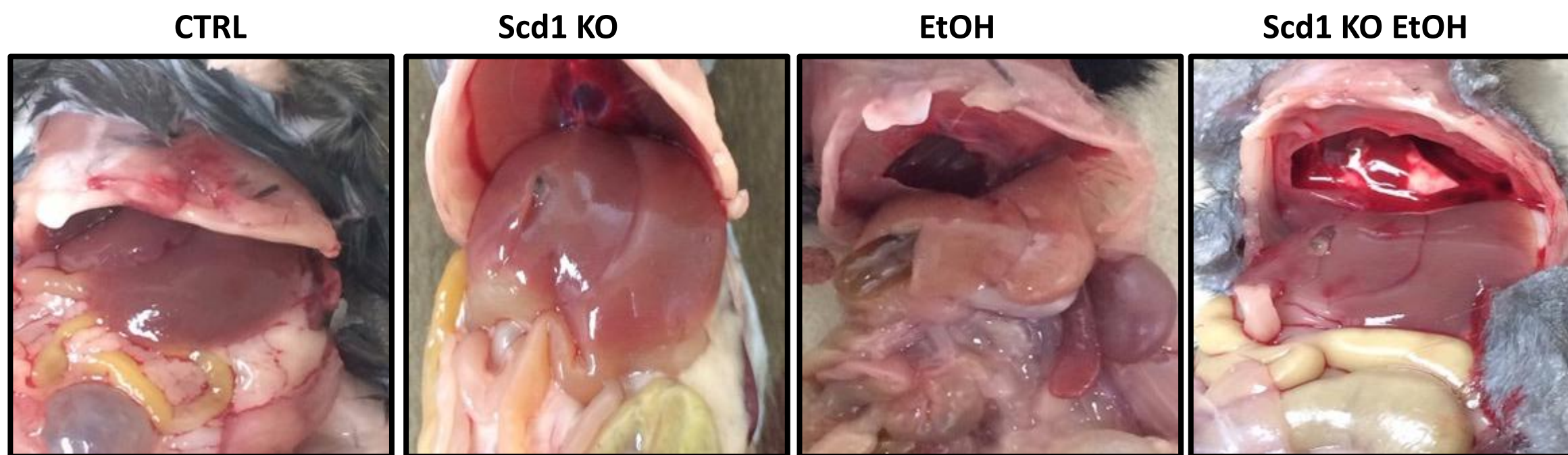
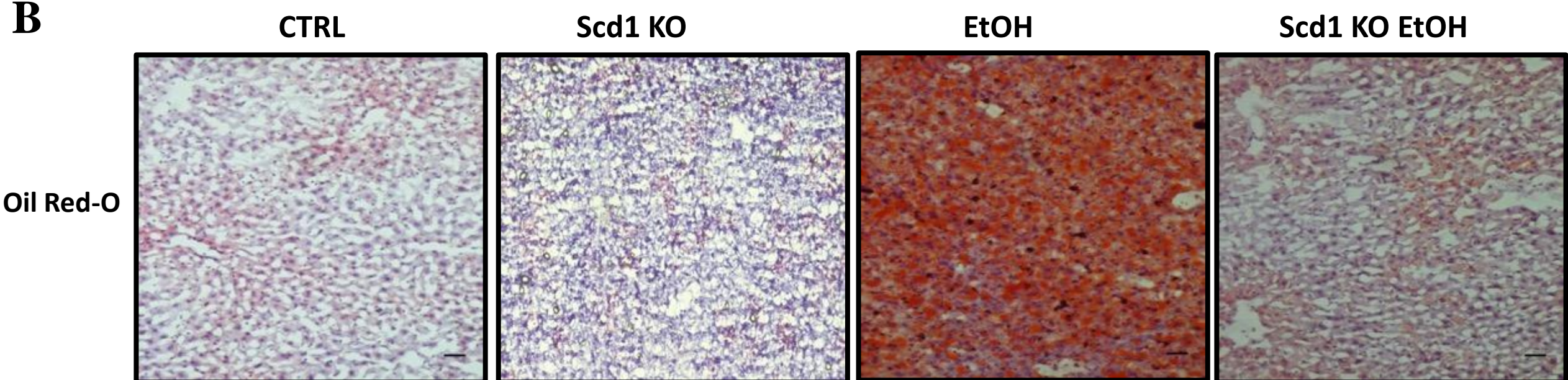
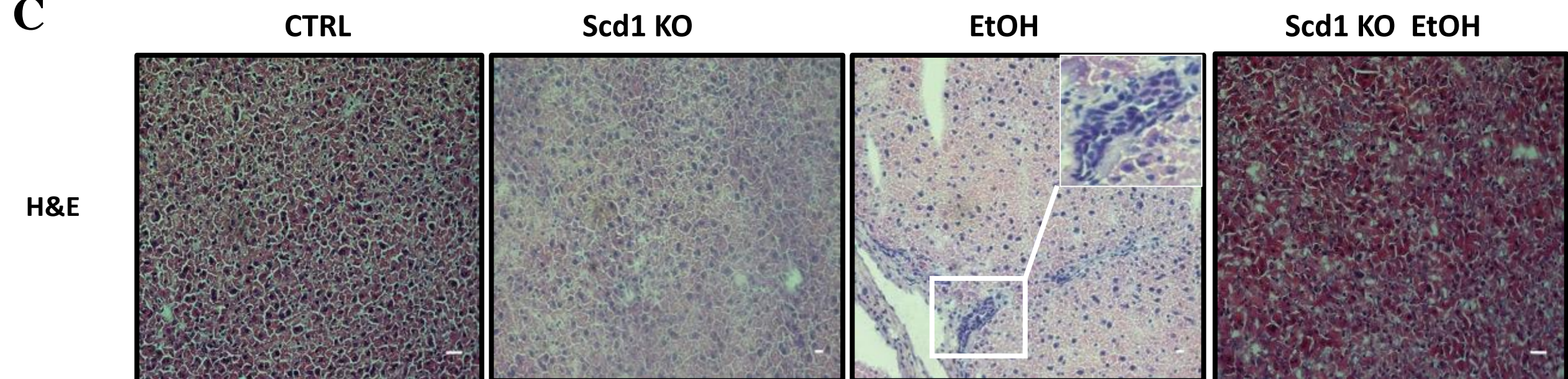
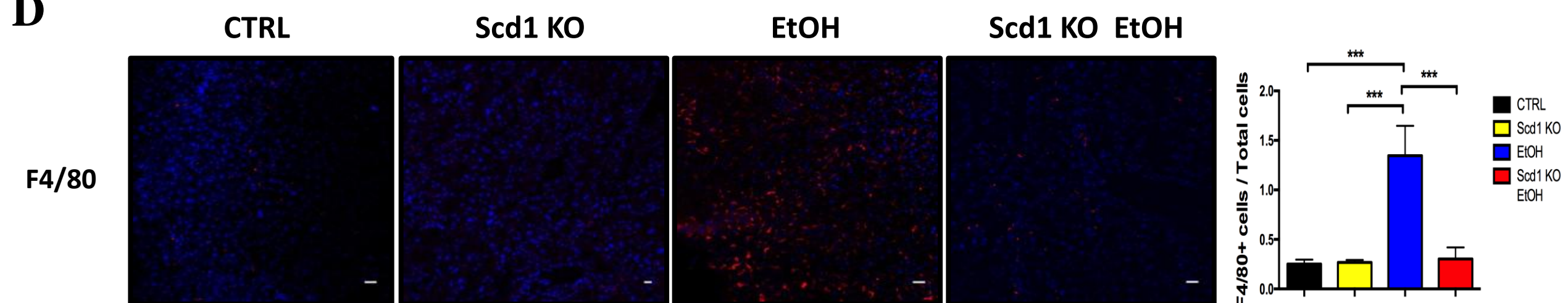
A**B****C****D**

Figure 2

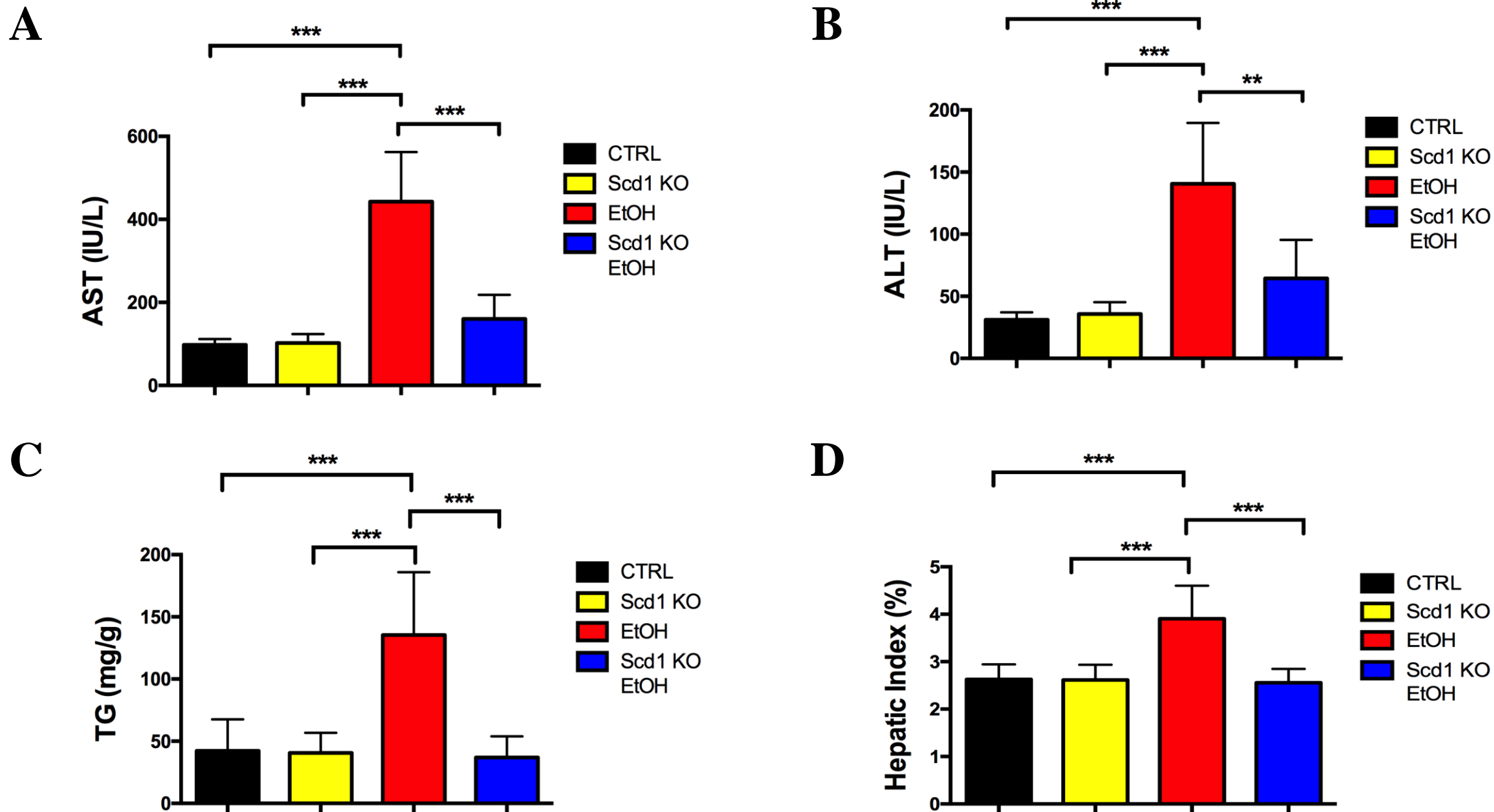
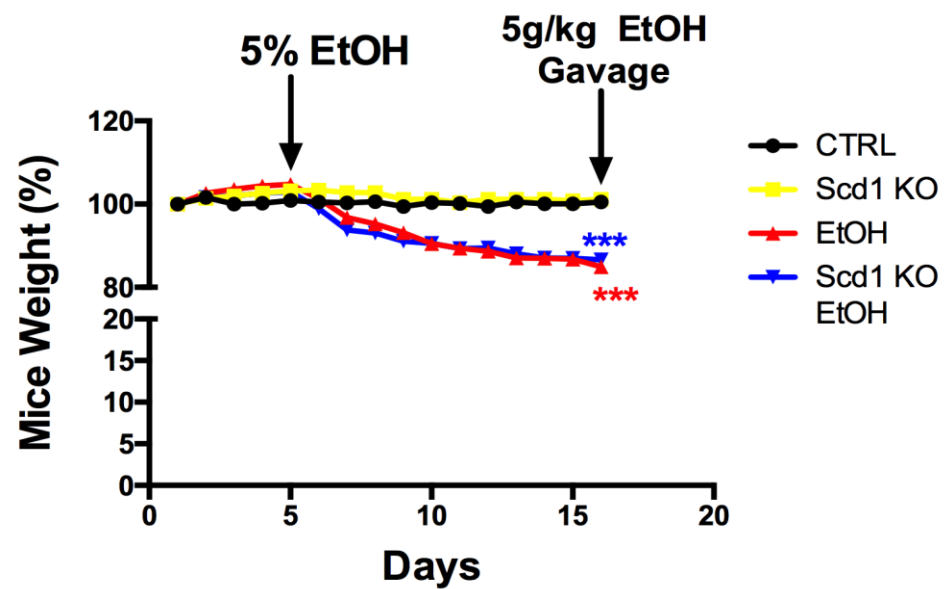
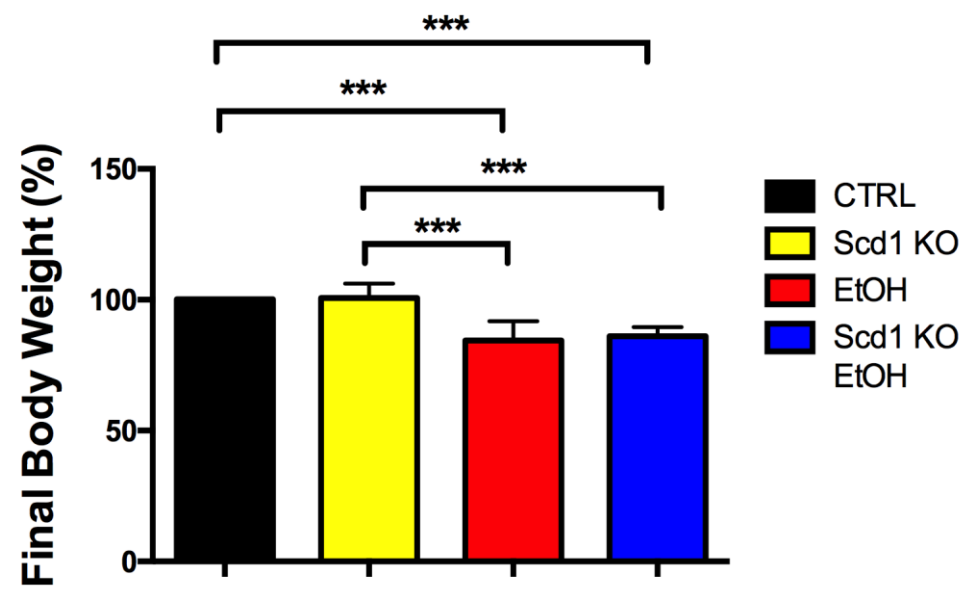


Figure 3

A



B



C

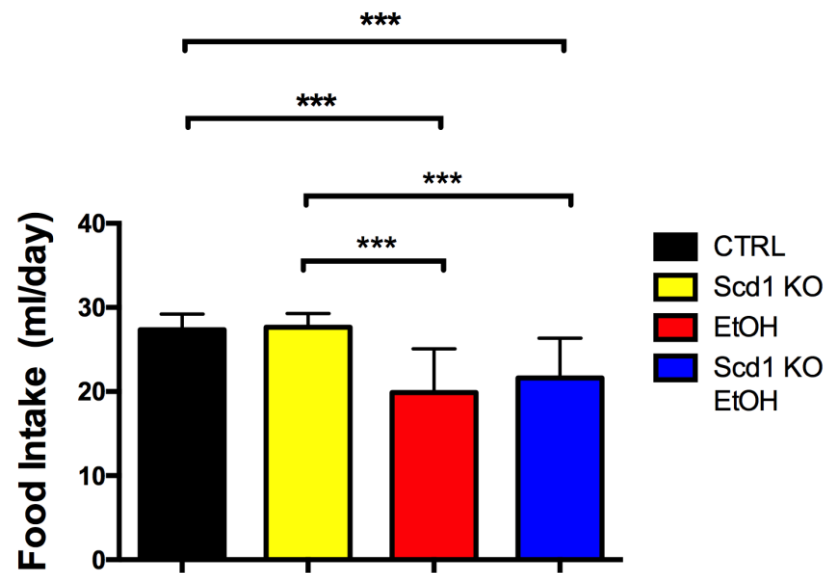
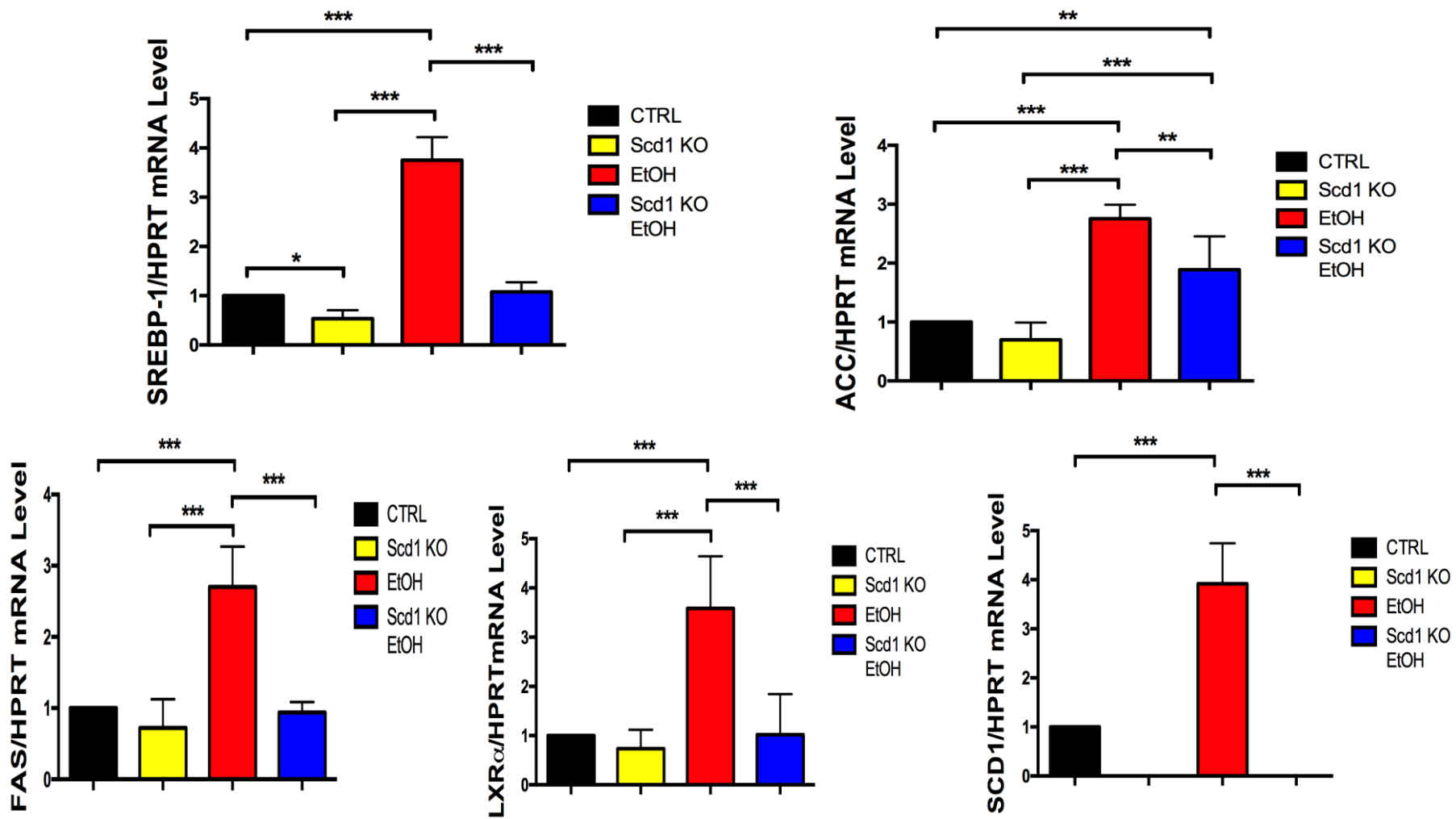


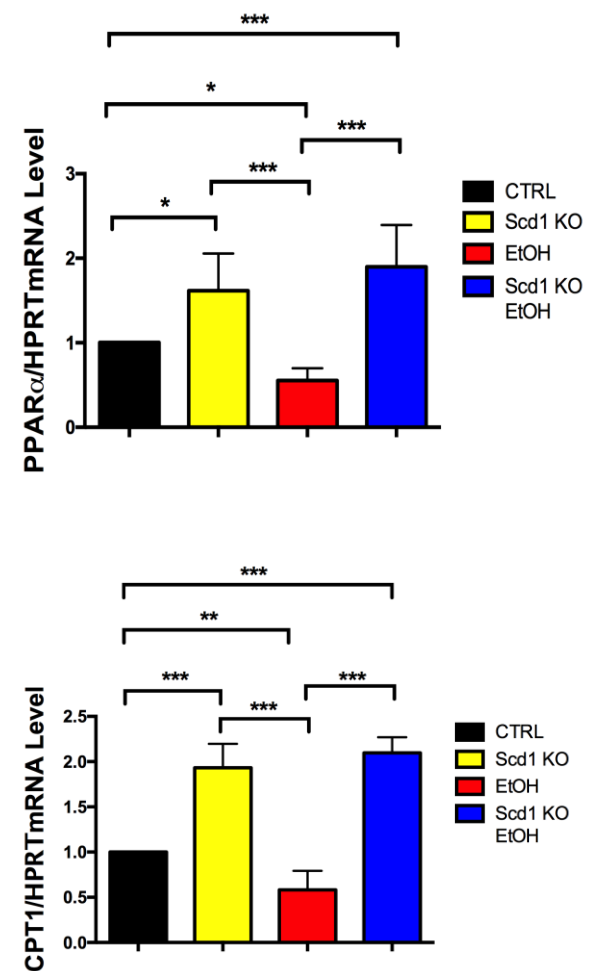
Figure 4

A



Lipogenesis

B



β -oxidation

Figure 5

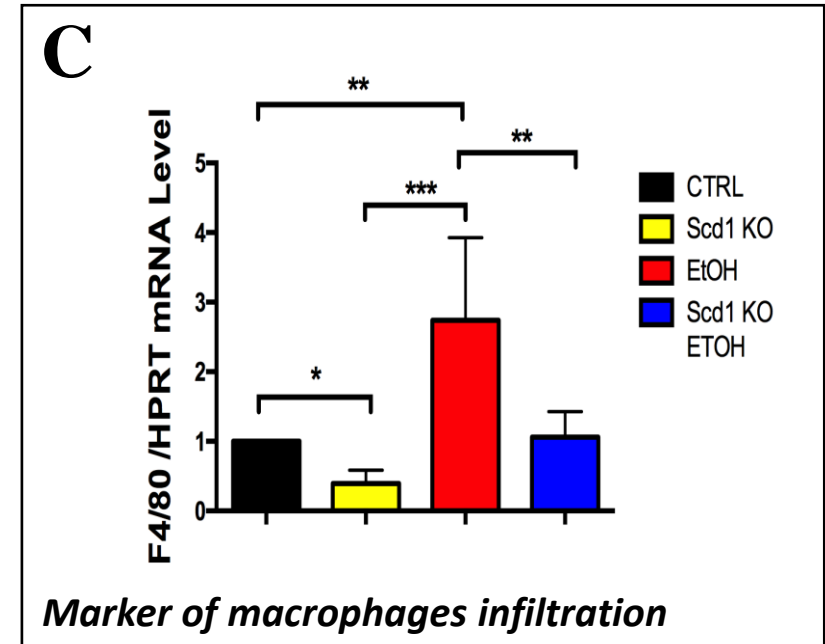
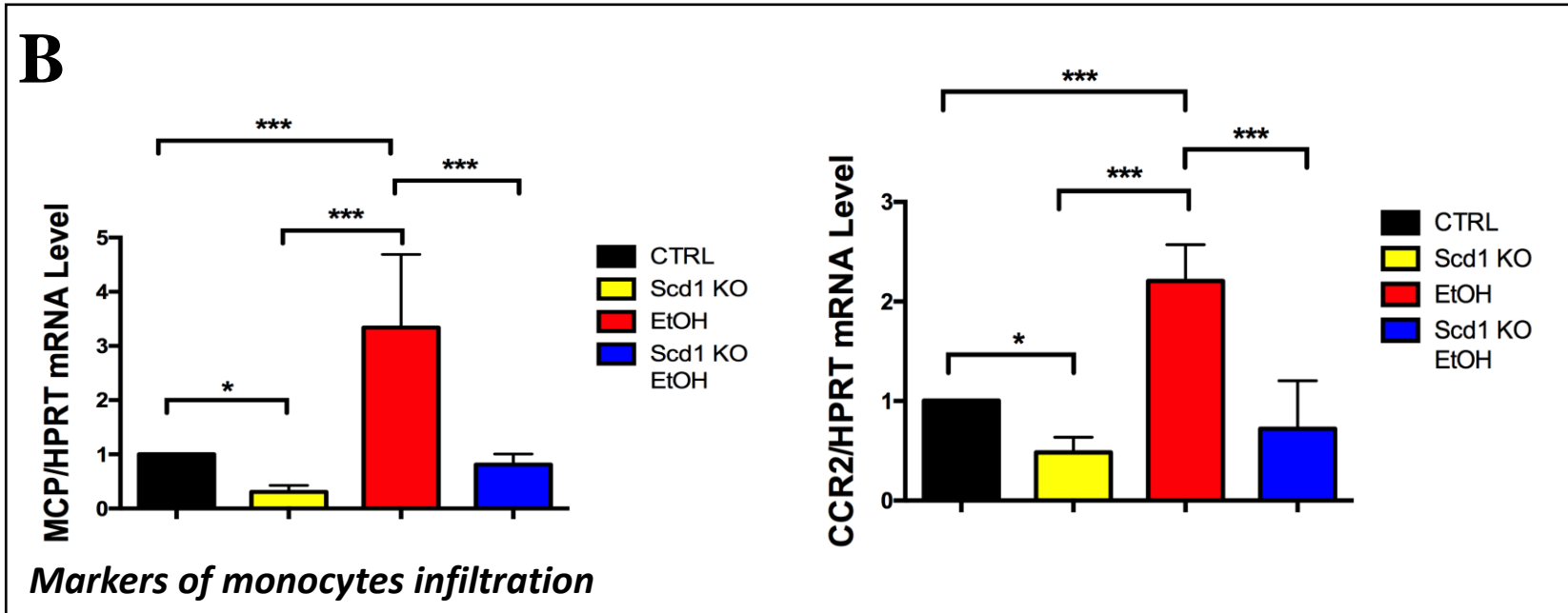
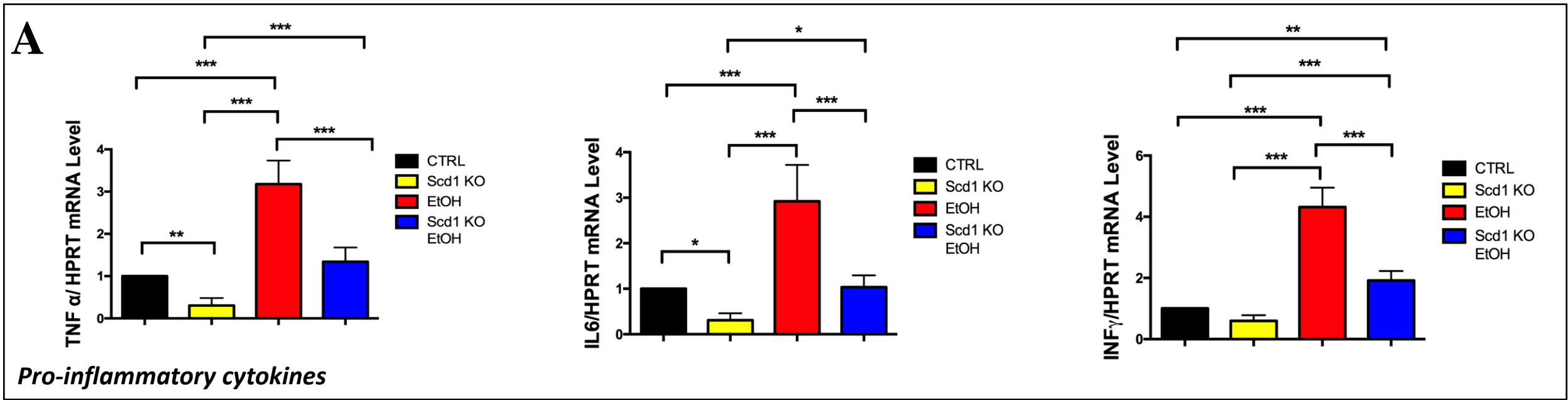


Figure 6

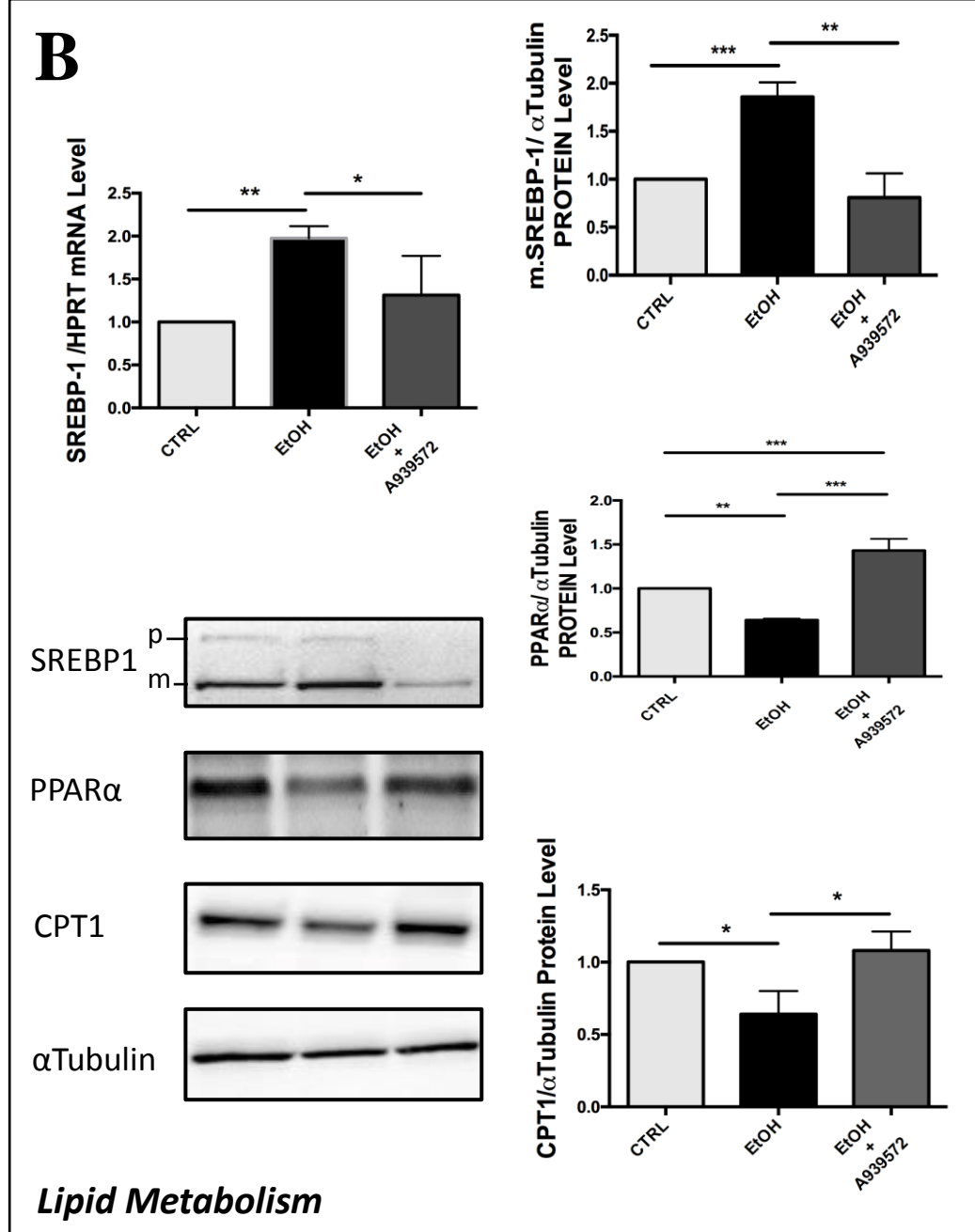
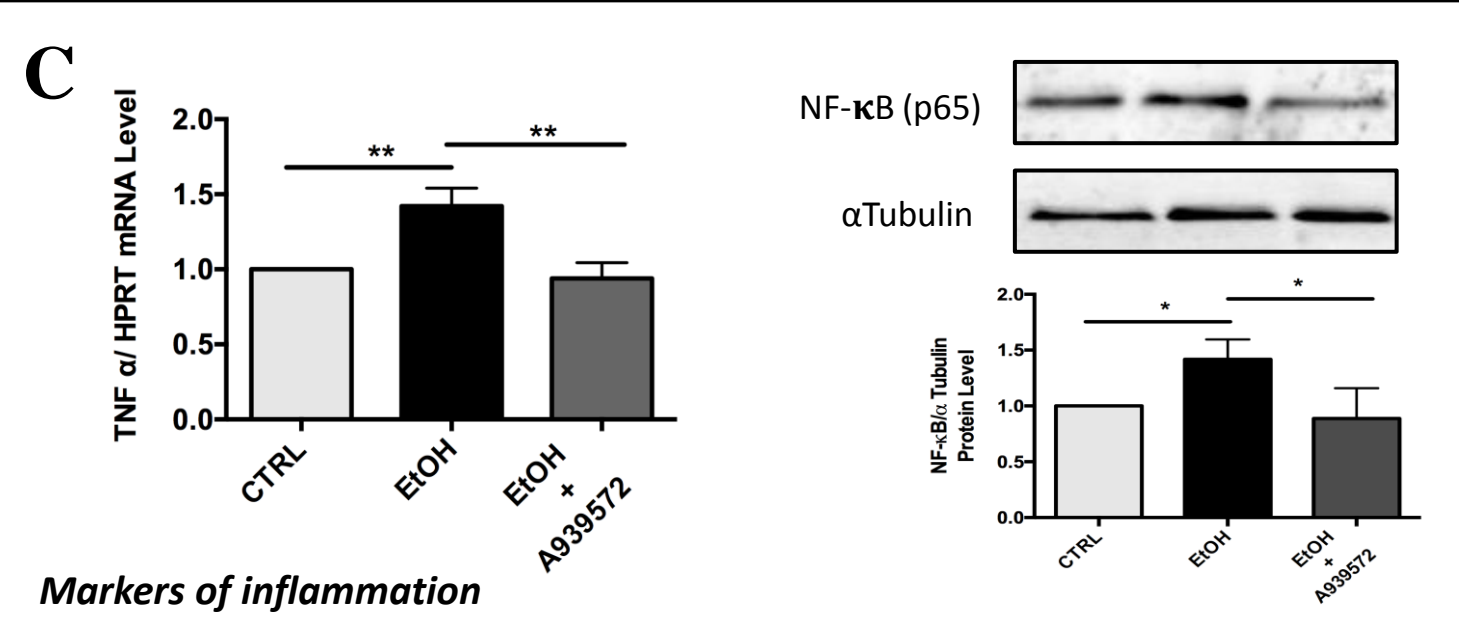
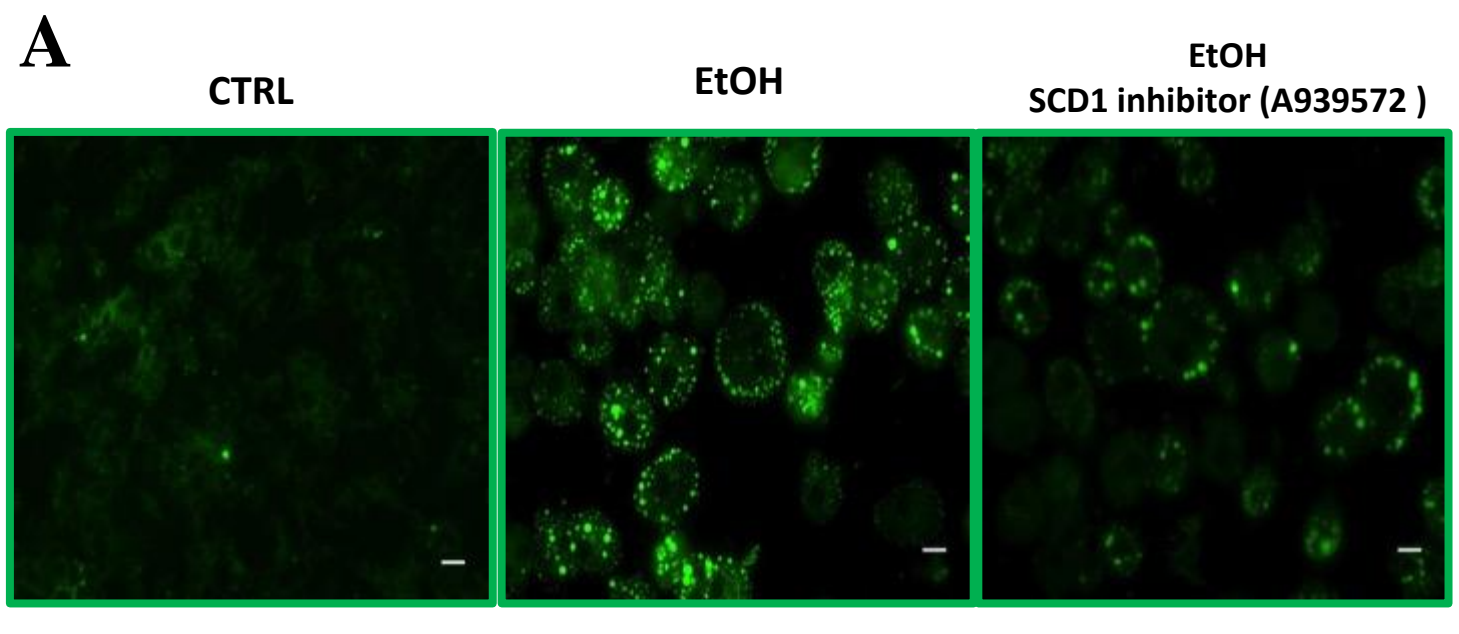
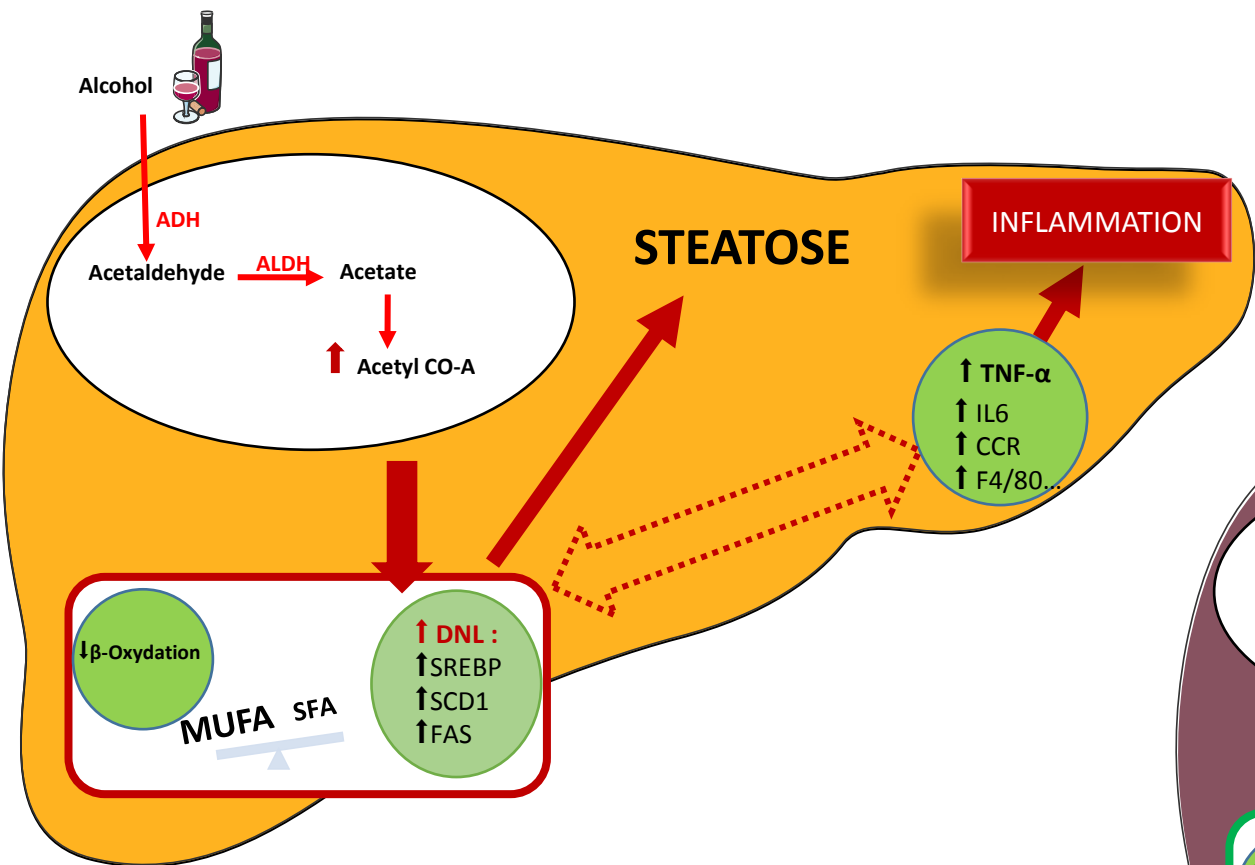


Figure 7

A



B

